



Supporting Online Material for

Measurement of the Entanglement of Two Superconducting Qubits via State Tomography

Matthias Steffen, M. Ansmann, Radoslaw C. Bialczak, N. Katz, Erik Lucero, R.
McDermott, Matthew Neeley, E. M. Weig, A. N. Cleland, John M. Martinis*

*To whom correspondence should be addressed. E-mail: martinis@physics.ucsb.edu

Published 8 September 2006, *Science* **313**, 1423 (2006)

DOI: 10.1126/science.1130886

This PDF file includes:

Materials and Methods
Figs. S1 and S2

Supporting Online Material

Phase Qubit. The design concepts behind this phase qubit have been discussed previously (11). A $\sim 1 \mu\text{m}^2$ area tunnel junction was shunted by a capacitor to reduce the effective density of two-level defects of the tunnel barrier, improving the coherence amplitude of the qubit (11). Amorphous silicon nitride was used for the dielectric material of the shunting capacitor: its loss tangent is consistent with the measured energy relaxation time. Parameters of the circuit are $C \sim 1.3 \text{ pF}$, $L \sim 850 \text{ pH}$, and $I_0 \sim 1.1 \mu\text{A}$. Inversion recovery and Rabi oscillations measurements for the individual qubits (driven separately when biased off resonance) are shown in Fig. S1. The qubit transition frequency $\omega_{10}/2\pi$ is sufficiently different from $\omega_{21}/2\pi$ ($(\omega_{10} - \omega_{21})/2\pi \sim 180 \text{ MHz}$) as to avoid any significant excitation of the $|2\rangle$ state (see Fig. 1B).

The two phase qubits are coupled via a 3 fF interdigitated capacitor, giving an interaction strength of $S/h = 10 \text{ MHz}$. Measurement crosstalk (5) between the qubits is expected to be insignificant because of the small interaction strength, as confirmed by measurements. An image of the two qubits is shown in Fig. S2.

Microwaves. The microwave pulses are generated using an IQ mixer. Phase and amplitude control is achieved by adding the signal of the two quadrature components (I and Q) of a continuous wave microwave signal, with separate amplitude control for each channel (11). One microwave source and two IQ mixers were used to achieve phase and amplitude control of the microwave pulses for both qubits.

State Tomography. Implementing state tomography requires calibration of the phase difference between the microwave pulses reaching the qubits, as the rotation axis depends on phase. Even if the same microwave pulse is generated by both mixers, the actual phase observed by the qubits differs because the microwave lines have slightly different lengths. Calibration of this phase offset is done in a separate experiment by simultaneously applying a 90_x pulse on qubit A and a 90_θ pulse on qubit B, where θ is an adjustable microwave phase angle. A plot of the

occupation probabilities versus free evolution time gives oscillations whose amplitude depends on the phase angle θ . The oscillation amplitudes of P_{01} and P_{10} are maximized (minimized) whenever the relative phase between the $|01\rangle$ and $|10\rangle$ states is 90 (0) degrees. When the oscillation amplitude is maximized and P_{10} peaks first, θ corresponds to a y -rotation for the second qubit and serves as our calibration.

The intrinsic occupation probabilities P_i for the two qubits can be inferred from the measured probabilities $P_M = (P_{00}, P_{01}, P_{10}, P_{11})^T$ and the measurement fidelities $F_0 = 0.95$ and $F_1 = 0.85$ (see text). The intrinsic occupation probabilities are computed as $P_i = F^{-1}P_M$ where

$$F = \begin{pmatrix} F_0^2 & F_0(1-F_1) & F_0(1-F_1) & (1-F_1)^2 \\ (1-F_0)F_0 & F_0F_1 & (1-F_0)(1-F_1) & (1-F_1)F_1 \\ (1-F_0)F_0 & (1-F_0)(1-F_1) & F_0F_1 & (1-F_1)F_1 \\ (1-F_0)^2 & (1-F_0)F_1 & (1-F_0)F_1 & F_1^2 \end{pmatrix} \quad (1)$$

We verified that none of the inferred intrinsic probabilities were negative. The measured probabilities were computed from 20,000 executions of the same experiment.

Figure S1

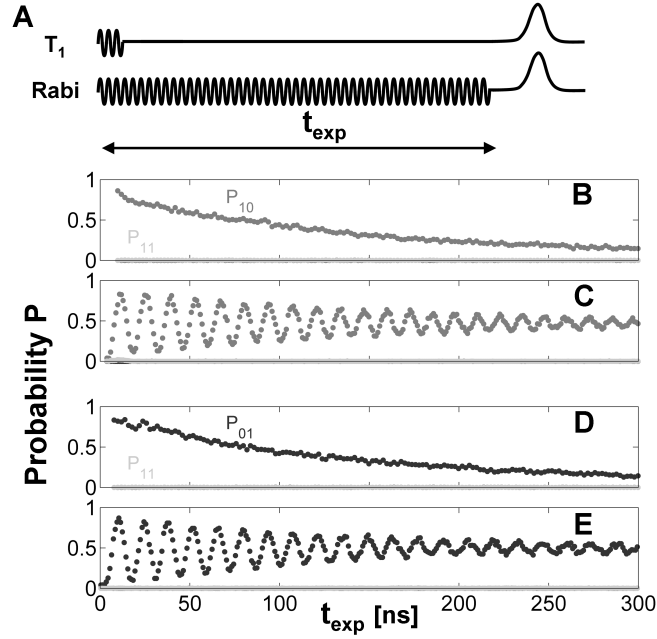


Figure 1: Inversion recovery (T_1) measurement and Rabi oscillations of the two phase qubits, each driven separately. (A) Control pulses for the experiment, including the final measure pulse, which are applied only to one of the qubits. While measuring one qubit, the other was biased far off resonance. (B,D) Inversion recovery (T_1) measurement for qubit A (B). The decay times are 130 ns, consistent with our single qubit experiment. (C,E) Rabi oscillations for qubit A (B). The visibility of the oscillations is $\sim 80\%$ and the dephasing time T_2^* (not shown) is found to be 80 ns for both qubits. No significant cross-talk is observed.

Figure S2

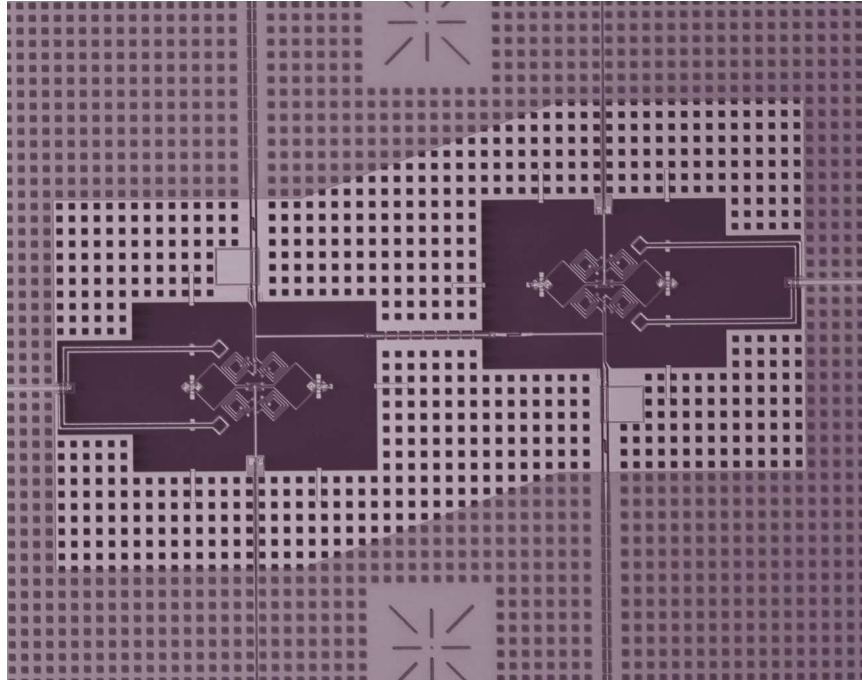


Figure 2: Micrograph image of the coupled qubits. The coupling capacitor linking the two qubits is just right of center. The shunting capacitor (white square), inductor (spiral) and SQUID (loops with crosses on them) are clearly visible. The qubit junction, located near the shunting capacitor, is not visible on this scale. The image size is 1.38 X 1.1 mm.